Material Model Library Manual

Bořek Patzák

Czech Technical University
Faculty of Civil Engineering
Department of Structural Mechanics
Thákurova 7, 166 29 Prague, Czech Republic

July 28, 2009

Contents

List of Tables

1 Material Models for Structural Analysis

1.1 Linear Elastic Materials

1.1.1 Isotropic Linear Elastic Material

Linear isotropic material model. The model parameters are summarized in table 1.

Description	Linear isotropic elastic material
Record Format	**IsoLE** $\text{num}_{(in)}$ # $\text{d}_{(rn)}$ # $\text{E}_{(rn)}$ # $\text{n}_{(rn)}$ # $\text{tAlpha}_{(rn)}$ #
Parameters	- *num* material model number - *d* material density - *E* Young modulus - *n* Poisson ratio - *tAlpha* thermal dilatation coefficient
Supported modes	3dMat, PlaneStress, PlaneStrain, 1dMat, 2dPlateLayer, 2dBeamLayer, 3dShellLayer, 2dPlate, 2dBeam, 3dShell, 3dBeam, PlaneStressRot
Features	Adaptivity support

Table 1: Linear Isotropic Material - summary.

1.1.2 Orthotropic Linear Elastic Material

Linear orthotropic, linear elastic material model. The model parameters are summarized in table 2. Local coordinate system, which determines axes of material orthotrophy can by specified using *lcs* array. This array contains six numbers, where first three numbers represent directional vector of local x-axis, and next three numbers represent directional vector of local y-axis. The local z-axis is determined using vector product. The right-hand coordinate system is assumed. Local coordinate system can also be specified using *scs* parameter. Then local coordinate system is specified in so called "shell" coordinate system, which is defined locally on each particular element and its definition is as follows: principal z-axis is perpendicular to shell mid-section, x-axis is perpendicular to z-axis and normal to user specified vector (so x-axis is parallel to plane, with being normal to this plane) and y-axis is perpendicular both to x and z axes. This definition of coordinate system can be used only with plates and shells elements. When vector is parallel to z-axis an error occurs. The *scs* array contain three numbers defining direction vector . If no local coordinate system is specified, by default a global coordinate system is used.

For 3D case the material compliance matrix has the following form

$$\boldsymbol{C} = \begin{bmatrix} 1/E_X & -\nu_{xy}/E_x & -\nu_{xz}/E_x & 0 & 0 & 0 \\ -\nu_{yx}/E_y & 1/E_y & -\nu_{yz}/E_y & 0 & 0 & 0 \\ -\nu_{zx}/E_z & -\nu_{zy}/E_z & 1/E_z & 0 & 0 & 0 \\ 0 & 0 & 0 & 1/G_{yz} & 0 & 0 \\ 0 & 0 & 0 & 0 & 1/G_{xz} & 0 \\ 0 & 0 & 0 & 0 & 0 & 1/G_{xy} \end{bmatrix} \tag{1}$$

By inversion, the material stiffness matrix has the form

$$\boldsymbol{D} = \begin{bmatrix} d_{xx} & d_{xy} & d_{xz} & 0 & 0 & 0 \\ & d_{yy} & d_{yz} & 0 & 0 & 0 \\ \text{sym} & & d_{zz} & 0 & 0 & 0 \\ 0 & 0 & 0 & G_{yz} & 0 & 0 \\ 0 & 0 & 0 & 0 & G_{xz} & 0 \\ 0 & 0 & 0 & 0 & 0 & G_{xy} \end{bmatrix} \tag{2}$$

where $\xi = 1 - (\nu_{xy} * \nu_{yx} + \nu_{yz} * \nu_{zy} + \nu_{zx} * \nu_{xz}) - (\nu_{xy} * \nu_{yz} * \nu_{zx} + \nu_{yx} * \nu_{zy} * \nu_{xz})$ and

$$\begin{aligned} d_{xx} &= E_X(1 - \nu_{yz} * \nu_{zy})/\xi, && (3)\\ d_{xy} &= E_y * (\nu_{xy} + \nu_{xz} * \nu_{zy})/\xi, && (4)\\ d_{xz} &= E_z * (\nu_{xz} + \nu_{yz} * \nu_{xy})/\xi, && (5)\\ d_{yy} &= E_y * (1 - \nu_{xz} * \nu_{zx})/\xi, && (6)\\ d_{yz} &= E_z * (\nu_{yz} + \nu_{yx} * \nu_{xz})/\xi, && (7)\\ d_{zz} &= E_z * (1 - \nu_{yx} * \nu_{xy})/\xi. && (8) \end{aligned}$$

E_i is the Young's modulus in the i-th direction, G_{ij} is the shear modulus in ij plane, ν_{ij} major Poisson's ratio, and ν_{ji} minor Poisson's ratio. Assuming that $E_x > E_y > E_z$, $\nu_{xy} > \nu_{yx}$ etc., then the ν_{xy} is refered to as major Poisson's ratio, while ν_{yx} refered as minor Poisson's ratio. Note, that there is only nine independent material parameters, because of symmetry conditions. The symmetry condition yields

$$\nu_{xy}E_y = \nu_{yx}E_x, \quad \nu_{yz}E_z = \nu_{zy}E_y, \quad \nu_{zx}E_x = \nu_{xz}E_z$$

The model description and parameters are summarized in table 2.

1.2 Plasticity Based Material Models

1.2.1 Drucker-Prager model

The Drucker-Prager plasticity model[1] is an isotropic elasto-plastic model based on a yield function

$$f(\boldsymbol{\sigma}, \tau_{\mathrm{Y}}) = F(\boldsymbol{\sigma}) - \tau_{\mathrm{Y}} \tag{9}$$

with the pressure-dependent equivalent stress

$$F(\boldsymbol{\sigma}) = \alpha I_1 + \sqrt{J_2} \tag{10}$$

As usual, $\boldsymbol{\sigma}$ is the stress tensor, τ_{Y} is the yield stress under pure shear, and I_1 and J_2 are the first invariant and second deviatoric invariant of the stress tensor. The friction coefficient α is a positive parameter that controls the influence of the pressure on the yield limit, important for cohesive-frictional materials such as concrete, soils or other geomaterials. The flow rule is derived from the plastic potential

$$g(\boldsymbol{\sigma}) = \alpha_\psi I_1 + \sqrt{J_2} \tag{11}$$

[1]Contributed by Simon Rolshoven, LSC, FENAC, EPFL.

Description	Orthotropic, linear elastic material
Record Format	**OrthoLE** num$_{(in)}$ # d$_{(rn)}$ # Ex$_{(rn)}$ # Ey$_{(rn)}$ # Ez$_{(rn)}$ # NYyz$_{(rn)}$ # NYxz$_{(rn)}$ # NYxy$_{(rn)}$ # Gyz$_{(rn)}$ # Gxz$_{(rn)}$ # Gxy$_{(rn)}$ # tAlphax$_{(rn)}$ # tAlphay$_{(rn)}$ # tAlphaz$_{(rn)}$ # [lcs$_{(ra)}$ #] [scs$_{(ra)}$ #]
Parameters	- *num* material model number - *d* material density - *Ex*, *Ey*, *Ez* Young moduluses for x,y, and z directions - *NYyz*, *NYxz*, *NYxy* major Poisson's ratio coefficients - *Gyz*, *Gxz*, *Gxy* Shear moduluses - *tAlphax*, *tAlphay*, *tAlphaz* thermal dilatation coefficients in x,y,z directions - *lcs* Array defining local material x and y axes of orthotrophy - *scs* Array defining a normal vector n. The local x axis is parallel to plane with n being plane normal. The material local z-axis is perpendicular to shell mid-section.
Supported modes	3dMat, PlaneStress, PlaneStrain, 1dMat, 2dPlateLayer, 2dBeamLayer, 3dShellLayer, 2dPlate, 2dBeam, 3dShell, 3dBeam, PlaneStressRot

Table 2: Orthotropic, linear elastic material - summary.

where α_ψ is the dilatancy coefficient. An associated model with $\alpha = \alpha_\psi$ would overestimate the dilatancy of concrete, so the dilatancy coefficient is usually chosen smaller than the friction coefficient. The model is described by the equations

$$\boldsymbol{\sigma} = \boldsymbol{D} : (\boldsymbol{\varepsilon} - \boldsymbol{\varepsilon}_\mathrm{p}) \tag{12}$$

$$\tau_\mathrm{Y} = h(\kappa) \tag{13}$$

$$\dot{\boldsymbol{\varepsilon}}_\mathrm{p} = \dot{\lambda}\frac{\partial g}{\partial \boldsymbol{\sigma}} = \dot{\lambda}\left(\alpha_\psi \boldsymbol{\delta} + \frac{\boldsymbol{s}}{2\sqrt{J_2}}\right) \tag{14}$$

$$\dot{\kappa} = \sqrt{\frac{2}{3}}\,\|\dot{\boldsymbol{\varepsilon}}_\mathrm{p}\| \tag{15}$$

$$\dot{\lambda} \geq 0, \quad f(\boldsymbol{\sigma}, \tau_\mathrm{Y}) \leq 0, \quad \dot{\lambda}\, f(\boldsymbol{\sigma}, \tau_\mathrm{Y}) = 0 \tag{16}$$

which represent the linear elastic law, hardening law, evolution laws for plastic strain and hardening variable, and the loading-unloading conditions. In the above, $\boldsymbol{D}$ is the elastic stiffness tensor, $\boldsymbol{\varepsilon}$ is the strain tensor, $\boldsymbol{\varepsilon}_\mathrm{p}$ is the plastic strain tensor, λ is the plastic multiplier, $\boldsymbol{\delta}$ is the unit second-order tensor, $\boldsymbol{s}$ is the deviatoric stress tensor, κ is the hardening variable, and a superior dot marks the derivative with respect to time. The flow rule has the form given in Eq. (14) at all points of the conical yield surface with the exception of its vertex, located on the hydrostatic axis.

For the present model, the evolution of the hardening variable can be explicitly linked to the plastic multiplier. Substituting the flow rule (14) into Eq. (15) and computing the norm leads to

$$\dot{\kappa} = k\dot{\lambda} \tag{17}$$

with a constant parameter $k = \sqrt{1/3 + 2\alpha_\psi^2}$, so the hardening variable is proportional to the plastic multiplier. For $\alpha = \alpha_\psi = 0$, the associated J_2-plasticity model is recovered as a special case.

In the simplest case of linear hardening, the hardening function is a linear function of κ, given by

$$h(\kappa) = \tau_0 + HE\kappa \tag{18}$$

where τ_0 is the initial yield stress, and H is the hardening modulus normalized with the elastic modulus. Alternatively, an exponential hardening function

$$h(\kappa) = \tau_{\text{limit}} + (\tau_0 - \tau_{\text{limit}})\, \mathrm{e}^{-\kappa/\kappa_c} \tag{19}$$

can be used for a more realistic description of hardening.

The stress-return algorithm is based on the Newton-iteration. In plasticity, this is commonly called Closest-Point-Projection (CPP), and it generally leads to quadratic convergence. The implemented algorithm is convergent in any stress case, but in the vicinity of the vertex region, quadratic convergence might be lost because of insufficient regularity of the yield function.

The algorithmic tangent stiffness matrix is implemented for both the regular case and the vertex region. Generally, the error decreases quadratically (of course only asymptotically). Again, in the vicinity of the vertex region, quadratic convergence might be lost due to insufficient regularity. Furthermore, the tangent stiffness matrix does not always exist for the vertex case. In these cases, the elastic stiffness is used instead. It is generally safer (but slower) to use the elastic stiffness if you encounter any convergence problems, especially if your problem is tension-dominated.

Description	DP material
Record Format	**druckerprager** num$_{(in)}$ # d$_{(rn)}$ # tAlpha$_{(rn)}$ # E$_{(rn)}$ # n$_{(rn)}$ # alpha$_{(rn)}$ # alphaPsi$_{(rn)}$ # ht$_{(in)}$ # iys$_{(rn)}$ # lys$_{(rn)}$ # hm$_{(rn)}$ # kc$_{(rn)}$ # [yieldtol$_{(rn)}$ #]
Parameters	- *num* material model number - *d* material density - *tAlpha* thermal dilatation coefficient - *E* Young modulus - *n* Poisson ratio - *alpha* friction coefficient - *alphaPsi* dilatancy coefficient - *ht* hardening type, 1: linear hardening, 2: exponential hardening - *iys* initial yield stress in shear, τ_0 - *lys* limit yield stress for exponential hardening, τ_{limit} - *hm* hardening modulus normalized with E-modulus (!) - *kc* κ_c for the exponential softening law - *yieldtol* tolerance of the error in the yield criterion, default value 1.e-14

Table 3: DP material - summary.

1.2.2 Composite plasticity model for masonry

Masonry is a composite material made of bricks and mortar. Nonlinear behavior of both components should be considered to obtain a realistic model able to describe cracking, slip, and crushing of the material. The model is based on paper by Lourenco and Rots [6]. It is formulated on the basis of softening plasticity for tension, shear, and compression (see fig.(1)). Numerical implementation is based on modern algorithmic concepts such as implicit integration of the rate equations and consistent tangent stiffness matrices.

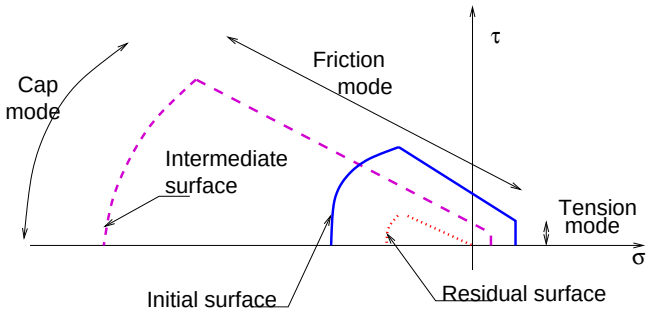

Figure 1: Composite yield surface model for masonry

The approach used in this work is based on idea of concentrating all the damage in the relatively weak joints and, if necessary, in potential tension cracks in the bricks. The joint interface constitutive model should include all important damage mechanisms. Here, the concept of interface elements is used. An interface element allows to incorporate discontinuities in the displacement field and its behavior is described in terms of a relation between the tractions and relative displacement across the interface. In the present work, these quantities will be denoted as $\boldsymbol{\sigma}$, generalized stress, and $\boldsymbol{\varepsilon}$, generalized strain. For 2D configuration, $\boldsymbol{\sigma} = \{\sigma, \tau\}^T$ and $\boldsymbol{\varepsilon} = \{u_n, u_s\}^T$, where σ and τ are the normal and shear components of the traction interface vector and n and s subscripts distinguish between normal and shear components of displacement vector. The

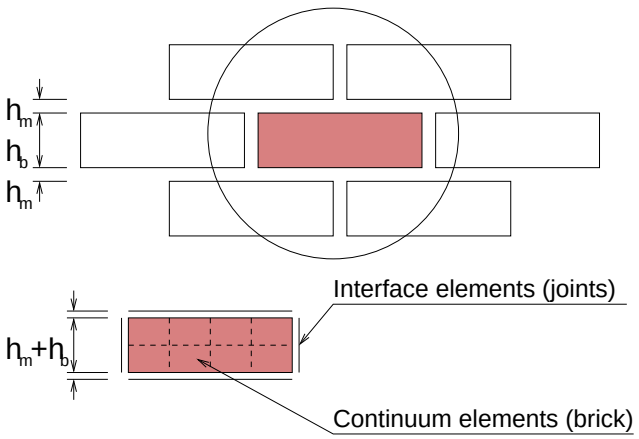

Figure 2: Modeling strategy for masonry

elastic response is characterized in terms of elastic constitutive matrix $\boldsymbol{D}$ as

$$\boldsymbol{\sigma} = \boldsymbol{D}\boldsymbol{\varepsilon} \tag{20}$$

For a 2D configuration $\boldsymbol{D} = diag\{k_n, k_s\}$. The terms of the elastic stiffness matrix can be obtained from the properties of both masonry and joints as

$$k_n = \frac{E_b E_m}{t_m(E_b - E_m)};\ k_s = \frac{G_b G_m}{t_m(G_b - G_m)} \tag{21}$$

where E_b and E_m are Young's moduli, G_b and G_m shear moduli for brick and mortar, and t_m is the thickness of joint. One should note, that there is no contact algorithm assumed between bricks, this means that the overlap of neighboring units will be visible. On the other hand, the interface model includes a compressive cap, where the compressive inelastic behavior of masonry is lumped.

Tension mode In the tension mode, the exponential softening law is assumed (see fig.(3)). The yield function has the following form

$$f_1(\boldsymbol{\sigma}, \kappa_1) = \sigma - f_t(\kappa_1) \tag{22}$$

where the yield value f_t is defined as

$$f_t = f_{t0} \exp\left(-\frac{f_{t0}}{G_f^I}\kappa_1\right) \tag{23}$$

The f_{t0} represents tensile strength of joint or interface; and G_f^I is mode-I fracture energy. For the tension mode, the associated flow hypothesis is assumed.

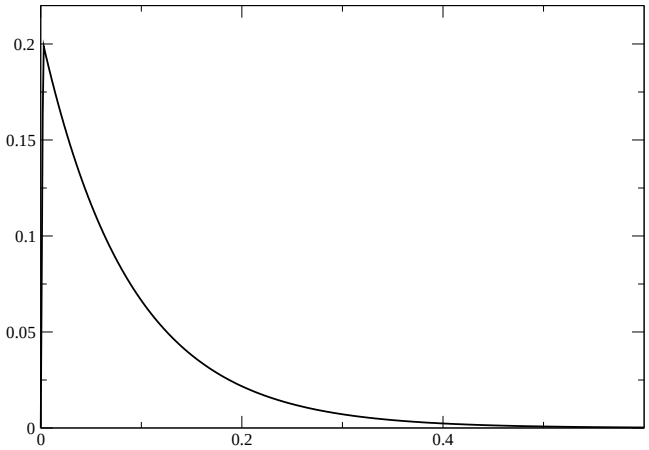

Figure 3: Tensile behavior of proposed model (f_t = 0.2 MPa, G_f^I = 0.018 N/mm)

Shear mode For the shear mode a Coulomb friction envelope is used. The yield function has the form

$$f_2(\boldsymbol{\sigma}, \kappa_2) = |\tau| + \sigma \tan\phi(\kappa_2) - c(\kappa_2) \tag{24}$$

According to [6] the variations of friction angle ϕ and cohesion c are assumed as

$$c = c_0 \exp\left(-\frac{c_0}{G_f^{II}}\kappa_2\right) \tag{25}$$

$$\tan\phi = \tan\phi_0 + (\tan\phi_r - \tan\phi_0)\left(\frac{c_0 - c}{c_0}\right) \tag{26}$$

where c_0 is initial cohesion of joint, ϕ_0 initial friction angle, ϕ_r residual friction angle, and G_f^{II} fracture energy in mode II failure. A non-associated plastic potential g_2 is considered as

$$g_2 = |\tau| + \sigma\tan\Phi - c \tag{27}$$

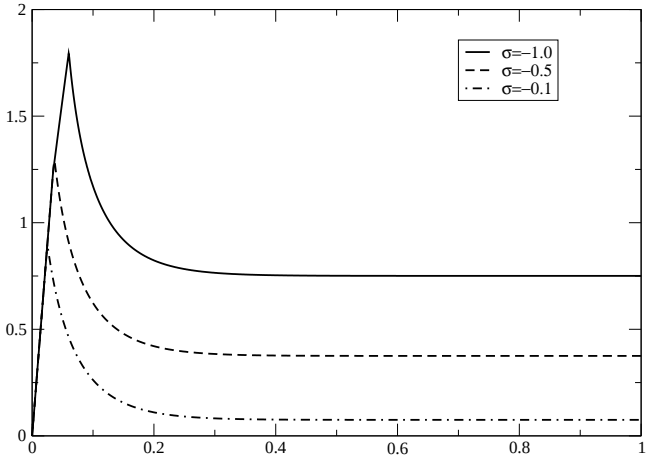

Figure 4: Shear behavior of proposed model for different confinement levels in MPa ($c_0 = 0.8$ MPa, $\tan\phi_0 = 1.0$, $\tan\phi_r = 0.75$, and $G_f^{II} = 0.05$ N/mm)

Coupling of tension/shear modes The tension and Coulomb friction modes are coupled with isotropic softening. This means that the percentage of softening in the cohesion is assumed to be the same as on the tensile strength

$$\dot\kappa_1 = \lambda_1 + \frac{G_f^I}{G_f^{II}}\frac{c_0}{f_{t0}}\lambda_2; \quad \dot\kappa_2 = \frac{G_f^{II}}{G_f^I}\frac{f_{t0}}{c_0}\lambda_1 + \lambda_2 \tag{28}$$

This follows from (23) and (25). However, in the corner region, when both yield surfaces are activated, such approach will lead to a non-acceptable penalty. For this reason a quadratic combination is assumed

$$\dot\kappa_1 = \sqrt{(\lambda_1)^2 + \left(\frac{G_f^I}{G_f^{II}}\frac{c_0}{f_{t0}}\lambda_2\right)^2}; \quad \dot\kappa_2 = \sqrt{\left(\frac{G_f^{II}}{G_f^I}\frac{f_{t0}}{c_0}\lambda_1\right)^2 + (\lambda_2)^2} \tag{29}$$

Cap mode For the cap mode, an ellipsoid interface model is used. The yield condition is assumed as

$$f_3(\boldsymbol{\sigma}, \kappa_3) = C_{nn}\sigma^2 + C_{ss}\tau^2 + C_n\sigma - \bar{\sigma}^2(\kappa_3) \tag{30}$$

where C_{nn}, C_{ss}, and C_n are material model parameters and $\bar{\sigma}$ is yield value, originally assumed in the following form of hardening/softening law [6]

$$\begin{aligned}
\bar{\sigma}_1(\kappa_3) &= \bar{\sigma}_i + (\bar{\sigma}_p - \bar{\sigma}_i)\sqrt{\frac{2\kappa_3}{\kappa_p} - \frac{\kappa_3^2}{\kappa_p^2}}; \;\; \kappa_3 \in (0, \kappa_p) \\
\bar{\sigma}_2(\kappa_3) &= \bar{\sigma}_p + (\bar{\sigma}_m - \bar{\sigma}_p)\left(\frac{\kappa_3 - \kappa_p}{\kappa_m - \kappa_p}\right)^2; \;\; \kappa_3 \in (\kappa_p, \kappa_m) \\
\bar{\sigma}_3(\kappa_3) &= \bar{\sigma}_r + (\bar{\sigma}_m - \bar{\sigma}_r)\exp\left(m\frac{\kappa_3 - \kappa_m}{\bar{\sigma}_m - \bar{\sigma}_r}\right); \;\; \kappa_3 \in (\kappa_m, \infty)
\end{aligned} \tag{31}$$

with $m = 2(\bar{\sigma}_m - \bar{\sigma}_p)/(\kappa_m - \kappa_p)$. The hardening/softening law (31) is shown in fig.(5). Note that the curved diagram is a C^1 continuous $\sigma - \kappa_3$ relation. The energy under the load-displacement diagram can be related to a "compressive fracture energy". The original hardening law (31.1) exhibits indefinite slope for $\kappa_3 = 0$, which can cause the problems with numerical implementation. This has been overcomed by replacing this hardening law with parabolic equation given by

$$\bar{\sigma}_1(\kappa_3) = \bar{\sigma}_i - 2 * (\bar{\sigma}_i - \bar{\sigma}_p) * \frac{\kappa_3}{\kappa_p} + (\bar{\sigma}_i - \bar{\sigma}_p)\frac{\kappa_3}{\kappa_p} \tag{32}$$

An associated flow and strain hardening hypothesis are being considered. This yields

$$\dot{\kappa}_3 = \lambda_3\sqrt{(2C_{nn}\sigma + C_n) * (2C_{nn}\sigma + C_n) + (2C_{ss}\tau) * (2C_{ss}\tau)} \tag{33}$$

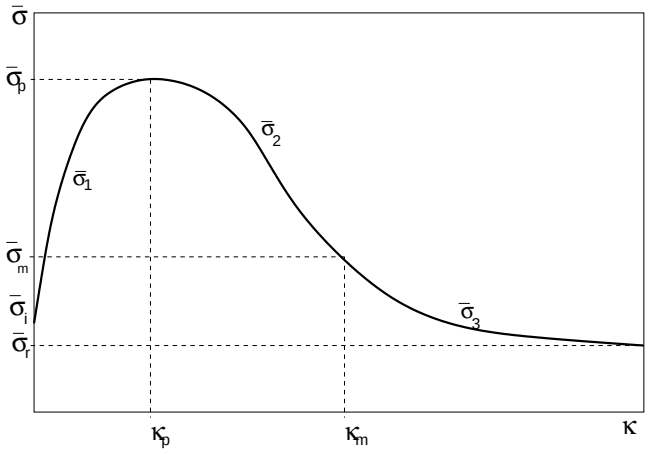

Figure 5: Hardening/softening law for cap mode

The model parameters are summarized in table 4. There is one algorithmic issue, that follows from the model formulation. Since the cap mode hardening/softening is not coupled to hardening/softening of shear and tension modes

the it may happen that when the cap and shear modes are activated, the return directions become parallel for both surfaces. This should be avoided by adjusting the input parameters accordingly (one can modify dilatancy angle, for example).

Description	Composite plasticity model for masonry
Record Format	**Masonry02** num$_{(in)}$ # d$_{(rn)}$ # E$_{(rn)}$ # n$_{(rn)}$ # ft0$_{(rn)}$ # gfi$_{(rn)}$ # gfii$_{(rn)}$ # kn$_{(rn)}$ # ks$_{(rn)}$ # c0$_{(rn)}$ # tanfi0$_{(rn)}$ # tanfir$_{(rn)}$ # tanpsi$_{(rn)}$ # si$_{(rn)}$ # sp$_{(rn)}$ # sm$_{(rn)}$ # sr$_{(rn)}$ # kp$_{(rn)}$ # km$_{(rn)}$ # kr$_{(rn)}$ # cnn$_{(rn)}$ # css$_{(rn)}$ # cn$_{(rn)}$ #
Parameters	- *num* material model number - *d* material density - *E* Young modulus - *n* Poisson ratio - *ft0* tensile strength - *gfi* fracture energy for mode I - *gfii* fracture energy for mode II - *kn* joint elastic property - *ks* joint elastic property - *c0* initial cohesion - *tanfi0* initial friction angle - *tanfir* residual friction angle - *tanpsi* dilatancy - $\{si,\ sp,\ sm,\ sr\}$ cap parameters $\{\bar{\sigma}_i, \bar{\sigma}_p, \bar{\sigma}_m, \bar{\sigma}_r\}$ - $\{kp,\ km, kr\}$ cap parameters $\{\kappa_p, \kappa_m, \kappa_r\}$ - *cnn,css,cn* cap mode parametrs
Supported modes	_2dInterface

Table 4: Composite model for masonry - summary.

1.2.3 HMH perfectly plastic material

Implements a perfectly plastic material. HMH plasticity condition with no hardening is used. Before plastic condition apply, and during unloading and reloading an isotropic linear elastic behavior is assumed. Linear elastic behavior is described using Young modulus and Poisson ratio. Plasticity condition is described using uniaxial strength. The model description and parameters are summarized in table 5.

1.2.4 Nonlinear elasto-plastic material model for concrete plates and shells

Nonlinear elasto-plastic material model with hardening. Takes into account uniaxial stress + transverse shear in concrete layers with transverse stirrups. Can be used only for 2d plates and shells with layered cross section and together with explicit integration method (stiffness matrix is not provided). The model description and parameters are summarized in table 6.

Description	HMH perfectly plastic material
Record Format	**Steel1** num$_{(in)}$ # d$_{(rn)}$ # E$_{(rn)}$ # n$_{(rn)}$ # tAlpha$_{(rn)}$ # Ry$_{(rn)}$ #
Parameters	- *num* material model number - *d* material density - *E* Young modulus - *n* Poisson ratio - *tAlpha* thermal dilatation coefficient - *Ry* uniaxial strength defining the yield limit
Supported modes	3dMat, PlaneStress, PlaneStrain, 1dMat, 2dPlateLayer, 2dBeamLayer, 3dShellLayer 3dBeam, PlaneStressRot

Table 5: HMH perfectly plastic material - summary.

1.2.5 J2 plasticity material model with hardening

1.3 Material models for tensile failure

1.3.1 Nonlinear elasto-plastic material model for concrete plates and shells

The description can be found is section 1.2.4.

1.3.2 Smeared rotating crack model

Implementation of smeared rotating crack model. Virgin material is modeled as isotropic linear elastic material (described by Young modulus and Poisson ratio). The onset of cracking begins, when principal stress reaches tensile strength. Further behavior is then determined by softening law, governed by principle of preserving of fracture energy G_f. For large elements, the tension strength can be artificially reduced to preserve fracture energy. Multiple cracks are allowed. The elastic unloading and reloading is assumed. In compression regime, this model correspond to isotropic linear elastic material. The model description and parameters are summarized in table 7.

1.3.3 Smeared rotating crack model with transition to scalar damage - linear softening

Implementation of smeared rotating crack model with transition to scalar damage with linear softening law. Improves the classical rotating model (see section 1.3.2) by introducing the transition to scalar damage model in later stages of tension softening.

Traditional smeared-crack models for concrete fracture are known to suffer by stress locking (meaning here spurious stress transfer across widely opening cracks), mesh-induced directional bias, and possible instability at late stages of the loading process. The combined model keeps the anisotropic character of the rotating crack but it does not transfer spurious stresses across widely open cracks. The new model with transition to scalar damage (RC-SD) keeps the anisotropic character of the RCM but it does not transfer spurious stresses across widely open cracks.

Description	Nonlinear elasto-plastic material model for concrete plates and shells
Record Format	**Concrete2** num$_{(in)}$ # d$_{(rn)}$ # E$_{(rn)}$ # n$_{(rn)}$ # SCCC$_{(rn)}$ # SCCT$_{(rn)}$ # EPP$_{(rn)}$ # EPU$_{(rn)}$ # EOPU$_{(rn)}$ # EOPP$_{(rn)}$ # SHEARTOL$_{(rn)}$ # IS_PLASTIC_FLOW$_{(in)}$ # IFAD$_{(in)}$ # STIRR_E$_{(rn)}$ # STIRR_Ft$_{(rn)}$ # STIRR_A$_{(rn)}$ # STIRR_TOL$_{(rn)}$ # STIRR_EREF$_{(rn)}$ # STIRR_LAMBDA$_{(rn)}$ #
Parameters	- *num* material model number - *d* material density - *E* Young modulus - *n* Poisson ratio - *SCCC* pressure strength - *SCCT* tension strength - *EPP* threshold effective plastic strain for softening in compression - *EPU* ultimate eff. plastic strain - *EOPP* threshold volumetric plastic strain for softening in tension - *EOPU* ultimate volumetric plastic strain - *SHEARTOL* threshold value of the relative shear deformation (psi**2/eef) at which shear is considered in layers. For lower relative shear deformations the transverse shear remains elastic decoupled from bending. default value SHEARTOL = 0.01 - *IS_PLASTIC_FLOW* indicates that plastic flow (not deformation theory) is used in pressure - *IFAD* State variables will not be updated, otherwise update state variables - *STIRR_E* Young modulus of stirrups - *STIRR_R* stirrups uniaxial strength = elastic limit - *STIRR_A* stirrups area/unit length (beam) or /unit area (shell) - *STIRR_TOL* stirrups tolerance of equilibrium in the z direction (=0 no iteration) - *STIRR_EREF* stirrups reference strain rate for Peryzna's material - *STIRR_LAMBDA* coefficient for that material (stirrups) - *SHTIRR_H* isotropic hardening factor for stirrups
Supported modes	3dShellLayer, 2dPlateLayer

Table 6: Nonlinear elasto-plastic material model for concrete - summary.

Virgin material is modeled as isotropic linear elastic material (described by Young modulus and Poisson ratio). The onset of cracking begins, when principal stress reaches tensile strength. Further behavior is then determined by **linear** softening law, governed by principle of preserving of fracture energy G_f. For large elements, the tension strength can be artificially reduced to preserve fracture energy. The transition to scalar damage model takes place,

Description	Rotating crack model for concrete
Record Format	**Concrete3** $d_{(rn)}$ # $E_{(rn)}$ # $n_{(rn)}$ # $Gf_{(rn)}$ # $Ft_{(rn)}$ # $exp\_soft_{(in)}$ # $tAlpha_{(rn)}$ #
Parameters	- *num* material model number - *d* material density - *E* Young modulus - *n* Poisson ratio - *Gf* fracture energy - *Ft* tension strength - *exp_soft* determines the type of softening, if nonzero exponential softening is used, linear otherwise - *tAlpha* thermal dilatation coefficient
Supported modes	3dMat, PlaneStress, PlaneStrain, 1dMat, 2dPlateLayer, 2dBeamLayer, 3dShellLayer

Table 7: Rotating crack model for concrete - summary.

when the softening stress reaches the specified limit. Multiple cracks are allowed. The elastic unloading and reloading is assumed. In compression regime, this model correspond to isotropic linear elastic material. The model description and parameters are summarized in table 8.

Description	RC-SD model for concrete
Record Format	**RCSD** $d_{(rn)}$ # $E_{(rn)}$ # $n_{(rn)}$ # $Gf_{(rn)}$ # $Ft_{(rn)}$ # $sdtransitioncoeff_{(rn)}$ # $tAlpha_{(rn)}$ #
Parameters	- *num* material model number - *d* material density - *E* Young modulus - *n* Poisson ratio - *Gf* fracture energy - *Ft* tension strength - *sdtransitioncoeff* determines the transition from RC to SD model. Transition takes plase when ratio of current softening stress to tension strength is less than *sdtransitioncoeff* value - *tAlpha* thermal dilatation coefficient
Supported modes	3dMat, PlaneStress, PlaneStrain, 1dMat, 2dPlateLayer, 2dBeamLayer, 3dShellLayer

Table 8: RC-SD model for concrete - summary.

1.3.4 Smeared rotating crack model with transition to scalar damage - exponential softening

Implementation of smeared rotating crack model with transition to scalar damage with exponential softening law. The description and model summary (table 9) are the same as for the RC-SD model with linear softening law (see section 1.3.3).

Description	RC-SD model for concrete with exponential softening law
Record Format	**RCSDE** $d_{(rn)}$ # $E_{(rn)}$ # $n_{(rn)}$ # $Gf_{(rn)}$ # $Ft_{(rn)}$ # sdtransitioncoeff$_{(rn)}$ # tAlpha$_{(rn)}$ #

Table 9: RC-SD model for concrete - summary.

1.3.5 Nonlocal Smeared rotating crack model with transition to scalar damage

Implementation of nonlocal version of smeared rotating crack model with transition to scalar damage. Improves the classical rotating model (see section 1.3.2) by introducing the transition to scalar damage model in later stages of tension softening. The improved RC-SD (see section 1.3.3) is further extended to a nonlocal formulation, which not only acts as a powerful localization limiter but also alleviates mesh-induced directional bias. A special type of material instability arising due to negative shear stiffness terms in the rotating crack model is resolved by switching to SD mode. A bell shaped nonlocal averaging function is used.

Virgin material is modeled as isotropic linear elastic material (described by Young modulus and Poisson ratio). The onset of cracking begins, when principal stress reaches tensile strength. Further behavior is then determined by **exponential** softening law.

The transition to scalar damage model takes place, when the softening stress reaches the specified limit or when the loss of material stability due to negative shear stiffness terms that may arise in the standard RCM formulation, which takes place when the ratio of minimal shear coefficient in stiffness to bulk material shear modulus reaches the limit.

Multiple cracks are allowed. The elastic unloading and reloading is assumed. In compression regime, this model correspond to isotropic linear elastic material. The model description and parameters are summarized in table 10.

1.3.6 Isotropic damage model in tension

This isotropic damage model assumes that the stiffness degradation is isotropic, i.e., stiffness moduli corresponding to different directions decrease proportionally and independently of direction of loading. The damaged stiffness tensor is expressed as $\boldsymbol{D} = (1-\omega)\boldsymbol{D}^e$. Damage evolution law is postulated in an explicit form, relating damage parameter and scalar measure of largest reached equivalent strain level in material e, taking into account the principle of preserving of fracture energy G_f. The equivalent strain, i.e., a scalar measure of the strain level is defined as norm from positive principal strains. The model description and parameters are summarized in table 11. The material uses crack-band approach to dissipate the correct annount of fracture energy by adjusting locally material parameters. There is a limit on element size, which can be expressed as

$$e0 \leq ef/l_e$$

where l_e is element length in the direction normal to crack plane, e0 is max effective strain at peak load, and ef is crack opening (not strain) when tension stress vanishes. This condition prevents a local snap-back of stress-strain diagram,

Description	RC-SD-NL model for concrete
Record Format	**RCSDNL** $d_{(rn)}$ # $E_{(rn)}$ # $n_{(rn)}$ # $Ft_{(rn)}$ # sdtransitioncoeff$_{(rn)}$ # sdtransitioncoeff2$_{(rn)}$ # $r_{(rn)}$ # tAlpha$_{(rn)}$ #
Parameters	- *num* material model number - *d* material density - *E* Young modulus - *n* Poisson ratio - *ef* deformation corresponding to fully open crack - *Ft* tension strength - *sdtransitioncoeff* determines the transition from RC to SD model. Transition takes place when ratio of current softening stress to tension strength is less than *sdtransitioncoeff* value - *sdtransitioncoeff2* determines the transition from RC to SD model. Transition takes place when ratio of current minimal shear stiffness term to virgin shear modulus is less than *sdtransitioncoeff2* value - *r* parameter specifying the width of nonlocal averaging zone - *tAlpha* thermal dilatation coefficient - *regionMap* map indicating the regions (currently region is characterized by cross section number) to skip for nonlocal avaraging. The elements and corresponding IP are not taken into account in nonlocal averaging process if corresponding regionMap value is nonzero.
Supported modes	3dMat, PlaneStress, PlaneStrain, 1dMat, 2dPlateLayer, 2dBeamLayer, 3dShellLayer

Table 10: RC-SD-NL model for concrete - summary.

which will otherwise occur to preserve correct amount of dissipated energy for large elements.

1.3.7 Nonlocal isotropic damage model in tension

Nonlocal version of isotropic damage model in tension. The nonlocal averaging acts as a powerful localization limiter. The bell-shaped nonlocal averaging function is used. The model description and parameters are summarized in table 12.

1.3.8 MDM - Anisotropic damage model

Local formulation The concept of isotropic damage is appropriate for materials weakened by voids, but if the physical source of damage is the initiation and propagation of microcracks, isotropic stiffness degradation can be considered only as a first rough approximation. More refined damage models take into account the highly oriented nature of cracking, which is reflected by the anisotropic character of the damaged stiffness or compliance matrices.

A number of anisotropic damage formulations have been proposed in the literature. Here we use a model outlined by M. Jirásek in [2], which is based on the

Description	Isotropic damage model for concrete in tension
Record Format	**idm1** $d_{(rn)}$ # $E_{(rn)}$ # $n_{(rn)}$ # $e0_{(rn)}$ # $ef_{(rn)}$ # $tAlpha_{(rn)}$ # $equivstraintype_{(in)}$ #
Parameters	- *num* material model number - *d* material density - *E* Young modulus - *n* Poisson ratio - *ef* crack opening (not strain) when tension stress vanishes - *e0* max effective strain at peak - *tAlpha* thermal dilatation coefficient - *equivstraintype* Allows to choose from different definitions of equivalent strain, which is a scalar measure of the strain level. The supported values are: 0- Mazar's definition of equivalent strain (default one) $\tilde{\varepsilon} = \sqrt{\sum_{I=1}^{3} <\varepsilon_I>^2}$, where $<\varepsilon_I>$ are positive parts of principal values of strain tensor, 1- corresponds to Rankine criterion of maximum principal stress and is based on the positive part of the effective stress ($\tilde{\varepsilon} = \frac{1}{E}\sqrt{\sum_{I=1}^{3} <\bar{\sigma}_I>^2}$), where $<\bar{\sigma}_I>$ are the positive parts of principal values of the effective stress tensor $\bar{\sigma} = \boldsymbol{D}_e : \varepsilon$, 2- equivalent strain defined as energy norm normalized by Young's modulus to obtain strain-like quantity ($\tilde{\varepsilon} = \sqrt{\frac{\varepsilon : \boldsymbol{D} : \varepsilon}{E}}$)
Supported modes	3dMat, PlaneStress, PlaneStrain, 1dMat
Features	Adaptivity support

Table 11: Isotropic Damage model in tension - summary.

principle of energy equivalence and on the construction of the inverse integrity tensor by integration of a scalar over all spatial directions. Since the model uses certain concepts from the microplane theory, it is called the microplane-based damage model (MDM).

The general structure of the MDM model is schematically shown in Fig. 6 and the basic equations are summarized in Table 13. Here, $\boldsymbol{\varepsilon}$ and $\boldsymbol{\sigma}$ are the (nominal) second-order strain and stress tensors with components $\boldsymbol{\varepsilon}_{ij}$ and σ_{ij}; $\boldsymbol{e}$ and $\boldsymbol{s}$ are first-order strain and stress tensors with components e_i and s_i, which characterize the strain and stress on "microplanes" of different orientations given by a unit vector $\boldsymbol{n}$ with components n_i; ψ is a dimensionless compliance parameter that is a scalar but can have different values for different directions $\boldsymbol{n}$; the symbol δ denotes a virtual quantity; and a sumperimposed tilde denotes an effective quantity, which is supposed to characterize the state

Description	Nonlocal isotropic damage model for concrete in tension
Record Format	**idmnl1** d$_{(rn)}$ # E$_{(rn)}$ # n$_{(rn)}$ # e0$_{(rn)}$ # ef$_{(rn)}$ # tAlpha$_{(rn)}$ #
Parameters	- *num* material model number - *d* material density - *E* Young modulus - *n* Poisson ratio - *ef* ε_f is a model parameter that controls the post-peak slope (the tangent modulus just after the peak is $E_t = -f_t/(\varepsilon_f - \varepsilon_0)$) - *e0* max effective strain at peak - *r* nonlocal interaction radius - *tAlpha* thermal dilatation coefficient - *regionMap* map indicating the regions (currently region is characterized by cross section number) to skip for nonlocal avaraging. The elements and corresponding IP are not taken into account in nonlocal averaging process if corresponding regionMap value is nonzero. - *equivstraintype* Allows to choose from different definitions of equivalent strain, which is a scalar measure of the strain level. For the description, see table 11.
Supported modes	3dMat, PlaneStress, PlaneStrain, 1dMat
Features	Adaptivity support

Table 12: Nonlocal isotropic Damage model in tension - summary.

of the intact material between defects such as microcracks or voids.

Table 13: Basic equations of microplane-based anisotropic damage model

$\tilde{\boldsymbol{e}} = \tilde{\boldsymbol{\varepsilon}} \cdot \boldsymbol{n}$	$\boldsymbol{s}^T = \psi \boldsymbol{s}$	$\boldsymbol{s} = \boldsymbol{\sigma} \cdot \boldsymbol{n}$
$\tilde{\boldsymbol{\sigma}} : \delta\tilde{\boldsymbol{\varepsilon}} = \dfrac{3}{2\pi} \displaystyle\int_\Omega \boldsymbol{s}^T \cdot \delta\tilde{\boldsymbol{e}} \, \mathrm{d}\Omega$	$\delta \boldsymbol{s} \cdot \boldsymbol{e} = d\boldsymbol{s}^T \cdot \tilde{\boldsymbol{e}}$	$\delta\boldsymbol{\sigma} : \boldsymbol{\varepsilon} = \dfrac{3}{2\pi} \displaystyle\int_\Omega \delta \boldsymbol{s} \cdot \boldsymbol{e} \, \mathrm{d}\Omega$
$\tilde{\boldsymbol{\sigma}} = \dfrac{3}{2\pi} \displaystyle\int_\Omega (\boldsymbol{s}^T \otimes \boldsymbol{n})_{\mathrm{sym}} \, \mathrm{d}\Omega$	$\boldsymbol{e} = \psi \tilde{\boldsymbol{e}}$	$\boldsymbol{\varepsilon} = \dfrac{3}{2\pi} \displaystyle\int_\Omega (\boldsymbol{e} \otimes \boldsymbol{n})_{\mathrm{sym}} \, \mathrm{d}\Omega$

Combining the basic equations, it is possible to show that the components of the damaged material compliance tensor are given by

$$C_{ijkl} = M_{pqij} M_{rskl} C^e_{pqrs} \tag{34}$$

where C^e_{pqrs} are the components of the elastic material compliance tensor,

$$M_{ijkl} = \tfrac{1}{4} \left(\psi_{ik}\delta_{jl} + \psi_{il}\delta_{jk} + \psi_{jk}\delta_{il} + \psi_{jl}\delta_{ik} \right) \tag{35}$$

are the components of the so-called damage effect tensor, and

$$\psi_{ij} = \frac{3}{2\pi} \int_\Omega \psi \, n_i n_j \, \mathrm{d}\Omega \tag{36}$$

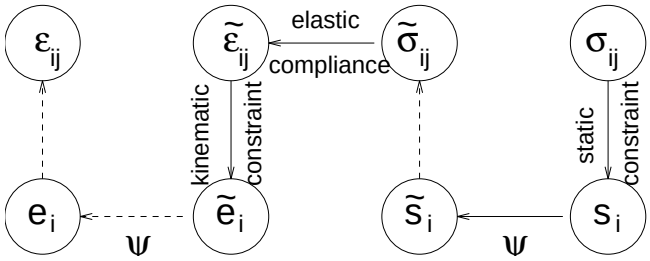

Figure 6: Structure of microplane-based anisotropic damage model

are the components of the second-order inverse integrity tensor. The integration domain Ω is the unit hemisphere. In practice, the integral over the unit hemisphere is evaluated by summing the contribution from a finite number of directions, according to one of the numerical integration schemes that are used by microplane models.

The scalar variable ψ characterizes the relative compliance in the direction given by the vector $\boldsymbol{n}$. If ψ is the same in all directions, the inverse integrity tensor evaluated from (36) is equal to the unit second-order tensor (Kronecker delta) multiplied by ψ, the damage effect tensor evaluated from (35) is equal to the symmetric fourth-order unit tensor multiplied by ψ, and the damaged material compliance tensor evaluated from (34) is the elastic compliance tensor multiplied by ψ^2. The factor multiplying the elastic compliance tensor in the isotropic damage model is $1/(1-\omega)$, and so ψ corresponds to $1/\sqrt{1-\omega}$. In the initial undamaged state, $\psi = 1$ in all directions. The evolution of ψ is governed by the history of the projected strain components. In the simplest case, ψ is driven by the normal strain $e_N = \boldsymbol{\varepsilon}_{ij} n_i n_j$. Analogy with the isotropic damage model leads to the damage law

$$\psi = f(\kappa) \tag{37}$$

and loading-unloading conditions

$$g(e_N, \kappa) \equiv e_N - \kappa \leq 0, \qquad \dot{\kappa} \geq 0, \qquad \dot{\kappa} g(e_N, \kappa) = 0 \tag{38}$$

in which κ is a history variable that represents the maximum level of normal strain in the given direction ever reached in the previous history of the material. An appropriate modification of the exponential softening law leads to the damage law

$$f(\kappa) = \begin{cases} 1 & \text{if } \kappa \leq e_0 \\ \sqrt{\frac{\kappa}{e_0} \exp\left(\frac{\kappa - e_0}{e_f - e_0}\right)} & \text{if } \kappa > e_0 \end{cases} \tag{39}$$

where e_0 is a parameter controlling the elastic limit, and $e_f > e_0$ is another parameter controlling ductility. Note that softening in a limited number of directions does not necessarily lead to softening on the macroscopic level, because the response in the other directions remains elastic. Therefore, e_0 corresponds to the elastic limit but not to the state at peak stress.

If the MDM model is used in its basic form described above, the compressive strength turns out to depend on the Poisson ratio and, in applications to

concrete, its value is too low compared to the tensile strength. The model is designed primarily for tensile-dominated failure, so the low compressive strength is not considered as a major drawback. Still, it is desirable to introduce a modification that would prevent spurious compressive failure in problems where moderate compressive stresses appear. The desired effect is achieved by redefining the projected strain e_N as

$$e_N = \frac{\boldsymbol{\varepsilon}_{ij} n_i n_j}{1 - \dfrac{m}{E e_0} \sigma_{kk}} \tag{40}$$

where m is a nonnegative parameter that controls the sensitivity to the mean stress, σ_{kk} is the trace of the stress tensor, and the normalizing factor Ee_0 is introduced in order to render the parameter m dimensionless. Under compressive stress states (characterized by $\sigma_{kk} < 0$), the denominator in (40) is larger than 1, and the projected strain is reduced, which also leads to a reduction of damage. A typical recommended value of parameter m is 0.05.

Nonlocal formulation Nonlocal formulation of the MDM model is based on the averaging of the inverse integrity tensor. This roughly corresponds to the nonlocal isotropic damage model with averaging of the compliance variable $\gamma = \omega/(1-\omega)$, which does not cause any spurious locking effects. In equation (35) for the evaluation of the damage effect tensor, the inverse integrity tensor is replaced by its weighted average with components

$$\bar{\psi}_{ij}(\boldsymbol{x}) = \int_V \alpha(\boldsymbol{x}, \boldsymbol{\xi}) \psi_{ij}(\boldsymbol{\xi}) \mathrm{d}\boldsymbol{\xi} \tag{41}$$

By fitting a wide range of numerical results, it has been found that the parameters of the nonlocal MDM model can be estimated from the measurable material properties using the formulas

$$\lambda_f = \frac{E G_f}{R f_t^2} \tag{42}$$

$$\lambda = \frac{\lambda_f}{1.47 - 0.0014 \lambda_f} \tag{43}$$

$$e_0 = \frac{f_t}{(1-m) E (1.56 + 0.006\lambda)} \tag{44}$$

$$e_f = e_0 [1 + (1-m)\lambda] \tag{45}$$

where E is Young's modulus, G_f is the fracture energy, f_t is the uniaxial tensile strength, m is the compressive correction factor, typically chosen as $m = 0.05$, and R is the radius of nonlocal interaction reflecting the internal length of the material.

Input Record The model description and parameters are summarized in table 14.

Description	MDM Anisotropic damage model
Record Format Parameters	Common parameters **mdm** d$_{(rn)}$ # nmp$_{(ins)}$ # talpha$_{(rn)}$ # parmd$_{(rn)}$ # nonloc$_{(in)}$ # formulation$_{(in)}$ # mode$_{(in)}$ # -*num* material model number - *D* material density - *nmp* number of microplanes used for hemisphere integration, supported values are 21,28, and 61 - *talpha* thermal dillatation coeff - *parmd* - *nonloc* - *formulation* - *mode*
Nonlocal variant I Additional params	 r$_{(rn)}$ # efp$_{(rn)}$ # ep$_{(rn)}$ # -*r* nonlocal interaction radius -*efp* $\varepsilon_f p$ is a model parameter that controls the post-peak slope $\varepsilon_f p = \varepsilon_f - \varepsilon_0$, where ε_f is strain at zero stress level. -*ep* max effective strain at peak ε_0
Nonlocal variant II Additional params	 r$_{(rn)}$ # gf$_{(rn)}$ # ft$_{(rn)}$ # -*r* nonlocal intraction radius -*gf* fracture energy -*ft* tensile strength
Local variant I Additional params	 efp$_{(rn)}$ # ep$_{(rn)}$ # -*efp* $\varepsilon_f p$ is a model parameter that controls the post-peak slope $\varepsilon_f p = \varepsilon_f - \varepsilon_0$, where ε_f is strain at zero stress level. -*ep* max effective strain at peak ε_0
Local variant II Additional params	 gf$_{(rn)}$ # ep$_{(rn)}$ # -*gf* fracture energy -*ep* max effective strain at peak ε_0
Supported modes Features	3dMat, PlaneStress Adaptivity support

Table 14: MDM model - summary.

1.4 Material models specific to concrete

1.4.1 Mazars damage model for concrete

This isotropic damage model assumes that the stiffness degradation is isotropic, i.e., stiffness moduli corresponding to different directions decrease proportionally and independently of direction of loading. It introduces two damage parameters ω_t and ω_c that are computed from the same equivalent strain using two different damage functions g_t and g_c. The g_t is identified from the uniaxial tension tests, while g_c from compressive test. The damage parameter for general stress states ω is obtained as a linear combination of ω_t and ω_c: $\omega = \alpha_t g_t + \alpha_c g_c$, where the coefficients α_t and α_c take into account the character of the stress state. The damaged stiffness tensor is expressed as $\boldsymbol{D} = (1-\omega)\boldsymbol{D}^e$. Damage evolution law is postulated in an explicit form, relating damage parameter and scalar measure of largest reached strain level in material, taking into account the principle of preserving of fracture energy G_f. The equivalent strain, i.e., a scalar measure of the strain level is defined as norm from positive principal strains. The model description and parameters are summarized in table 15.

Description	Mazars damage model for concrete
Record Format	**mazarsmodel** d(rn) # E(rn) # n(rn) # e0(rn) # ac(rn) # bc(rn) # beta(rn) # hreft(rn) # hrefc(rn) # version(in) # at(rn) # [bt(rn) #] tAlpha(rn) #
Parameters	- *num* material model number - *d* material density - *E* Young modulus - *n* Poisson ratio - *tAlpha* thermal dilatation coefficient - *version* Model variant. if 0 specified, the original form $g_t = 1.0 - (1.0 - A_t) * \varepsilon_0/\kappa - A_t * \exp(-B_t * (\kappa - \varepsilon_0))$; of tension damage evolution law is used, if equal 1, the modified law used which asymptotically tends to zero $g_t = 1.0 - (\varepsilon_0/\kappa) * \exp((\varepsilon_0 - \kappa)/A_t)$ - *ac*,*bc* material parameters related to the shape of uniaxial compression curve (A sample set used by Saouridis is $A_c = 1.34, B_c = 2537$ - *at*, [*bt*] material parameters related to the shape of uniaxial tension curve. Meaning dependent on *version* parameter. - *beta* coefficient reducing the effect of damage under response under shear. Default value set to 1.06 - *hreft*, *hrefc* reference characteristic lengths for tension and compression. The material parameters are specified for element with these characteristic lengths. The current element then will have the same COD (Crack Opening Displacement) as reference one.
Supported modes	3dMat, PlaneStress, PlaneStrain, 1dMat

Table 15: Mazars Damage model - summary.

1.4.2 Nonlocal Mazars damage model for concrete

The nonlocal variant of Mazars damage model for concrete. Model based on nonlocal averaging of equivalent strain. The nonlocal averaging acts as a powerful localization limiter. The bell-shaped nonlocal averaging function is used. The model description and parameters are summarized in table 16.

Description	Nonlocal Mazars damage model for concrete
Record Format	**mazarsmodelnl** $r_{(rn)}$ # $E_{(rn)}$ # $n_{(rn)}$ # $e0_{(rn)}$ # $ac_{(rn)}$ # $bc_{(rn)}$ # $beta_{(rn)}$ # $version_{(in)}$ # $at_{(rn)}$ # [$bt_{(rn)}$ #] $r_{(rn)}$ # $tAlpha_{(rn)}$ #
Parameters	- *num* material model number - *d* material density - *E* Young modulus - *n* Poisson ratio - *tAlpha* thermal dilatation coefficient - *version* Model variant. if 0 specified, the original form $g_t = 1.0 - (1.0 - A_t) * \varepsilon_0/\kappa - A_t * \exp(-B_t * (\kappa - \varepsilon_0))$; of tension damage evolution law is used, if equal 1, the modified law used which asymptotically tends to zero $g_t = 1.0 - (\varepsilon_0/\kappa) * \exp((\varepsilon_0 - \kappa)/A_t)$ - *ac*,*bc* material parameters related to the shape of uniaxial compression curve (A sample set used by Saouridis is $A_c = 1.34, B_c = 2537$ - *at*, [*bt*] material parameters related to the shape of uniaxial tension curve. Meaning dependent on *version* parameter. - *beta* coefficient reducing the effect of damage under response under shear. Default value set to 1.06 - *r* parameter specifying the width of nonlocal averaging zone
Supported modes	3dMat, PlaneStress, PlaneStrain, 1dMat

Table 16: Nonlocal Mazars Damage model - summary.

1.4.3 CebFip78 model for concrete aging

Implementation of CebFip78 material model for concrete aging. The model description and parameters are summarized in table 17.

1.4.4 DoublePowerLaw model for concrete aging

Implementation of CebFip78 material model for concrete aging. The model description and parameters are summarized in table 18.

1.4.5 B3 model for concrete aging

Implementation of B3 material model for concrete aging. The model description and parameters are summarized in table 19.

Description	CebFip78 Material model for concrete aging
Record Format	**CebFip78** $n_{(rn)}$ # relMatAge$_{(rn)}$ # E28$_{(rn)}$ # fibf$_{(rn)}$ # kap_a$_{(rn)}$ # kap_c$_{(rn)}$ # kap_tt$_{(rn)}$ # u$_{(rn)}$ #
Parameters	- *num* material model number - *E28* Young modulus at age of 28 days [MPa] - *n* Poisson ratio - *fibf* basic creep coefficient - *kap_a* coefficient of hydrometric conditions - *kap_c* coefficient of type of cement - *kap_tt* coeficient of temperature effects - *u* surface imposed to environment $[mm^2]$; temporary here; should be in crosssection level - *relmatage* relative material age
Supported modes	3dMat, PlaneStress, PlaneStrain, 1dMat, 2dPlateLayer,2dBeamLayer, 3dShellLayer

Table 17: CebFip78 Material model - summary.

Description	Double power law - like material model for concrete aging
Record Format	**doublepowerlaw** $n_{(rn)}$ # relMatAge$_{(rn)}$ # E28$_{(rn)}$ # fi1$_{(rn)}$ # m$_{(rn)}$ # n$_{(rn)}$ # alpha$_{(rn)}$ #
Parameters	- *num* material model number - *E28* Young modulus at age of 28 days [MPa] - *n* Poisson ratio - *fibf* basic creep coefficient - *m* coefficient - *n* coefficient - *alpha* coeficient - *relmatage* relative material age
Supported modes	3dMat, PlaneStress, PlaneStrain, 1dMat, 2dPlateLayer,2dBeamLayer, 3dShellLayer

Table 18: Double power law material model - summary.

1.4.6 Microplane model M4

Implementation of Microplane model M4. This model is based on microplane concept. It describes the complex 3d behavior of material. However, the objectivity of model with regard to element size is unsolved - the parameters should be fitted for each element size. Since the stiffness matrix is not provided, a linear elastic is provided. This cause very slow convergence, when used in implicit codes. The model description and parameters are summarized in table 20.

Description	B3 material model for concrete aging
Record Format	**B3mat** n(rn) # relMatAge(rn) # fc(rn) # cc(rn) # w/c(rn) # a/c(rn) # t0(rn) # alpha1(rn) # alpha2(rn) # ks(rn) # hum(rn) # vs(rn) # noshrinkage(in) #
Parameters	- *num* material model number - *n* Poisson ratio - *relmatage* relative material age - *fc* 28-day standard cylinder compression strength in MPa - *cc* cement content of concrete in kg m^-3 - *w/c* ratio (by weight) of water to cementitious material - *a/c* ratio (by weight) of aggregate to cement - *t0* age when drying begins (in days) - *alpha1*,*alpha2* shrinkage parameters - *ks* cross section shape factor - *hum* relative humidity of the environment - *vs* volume to surface ratio (in m) - *noshrinkage* flag, if nonzero shrinkage is not taken into account
Supported modes	3dMat, PlaneStress, PlaneStrain, 1dMat, 2dPlateLayer,2dBeamLayer, 3dShellLayer

Table 19: B3 material model - summary.

Description	M4 material model
Record Format	**microplane_m4** nmp(in) # c3(rn) # c20(rn) # k1(rn) # k2(rn) # k3(rn) # k4(rn) # E(rn) # n(rn) #
Parameters	- *nmp* number of microplanes, supported values are 21, 28 and 61 - *n* Poisson ratio - *E* Young modulus - *c3*,*c20*, *k1*, *k2*, *k3*, *k4* model parameters
Supported modes	3dMat

Table 20: M4 - summary.

1.5 Material model for composite brittle damage

The model is designed for transversely isotropic elastic material defined by five elastic material constants. Axis 1 represents the principal direction. The relation to orthotropic material reads

$$\nu_{12} = \nu_{13},\ \nu_{21} = \nu_{31},\ \nu_{23} = \nu_{32},\ E_{22} = E_{33} \tag{46}$$

$$G_{12} = G_{13} = G_{21} = G_{31}, G_{23} = G_{32} \tag{47}$$

$$\frac{\nu_{12} = \nu_{13}}{E_{11}} = \frac{\nu_{21} = \nu_{31}}{E_{22}},\ \frac{\nu_{31} = \nu_{21}}{E_{33}} = \frac{\nu_{13} = \nu_{12}}{E_{11}} \tag{48}$$

Material orientation on finite element can be specified with *mlcs* optional parameter. If unspecified, material orientation is the same as the global coordinate system. This array contains six numbers, where first three numbers represent directional vector of local x-axis, and next three numbers represent directional vector of local y-axis with the reference to the global coordinate system. The composite material is extended to 1d and is suitable for trusses. In such particular case, only xx components are considered from material definition.

The linear softening occurs after reaching a critical stress f_t in mode I, see Fig. 7. Orientation of cracks is assumed to be orthogonal and aligned with orientation of material axis [7, pp.236]. The transverse isotropy is generally lost upon fracture, material becomes orthotropic and six damage parameters $d_1, d_2, \ldots d_6$ are introduced.

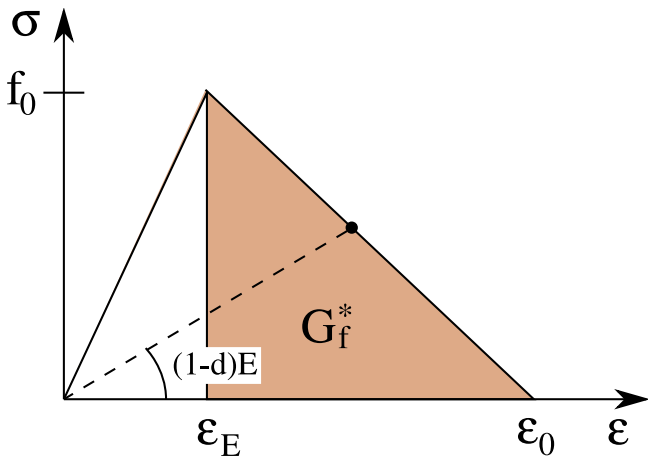

Figure 7: Implemented stress-strain evolution with damage for 1D case. Tension and compression are separated, but sharing the same damage parameter.

The compliance matrix, in the secant form and including damage parameters, reads

$$\begin{bmatrix} \frac{1-d_1}{E_{11}} & -\frac{\nu_{21}}{E_{22}} & -\frac{\nu_{31}}{E_{33}} & 0 & 0 & 0 \\ -\frac{\nu_{12}}{E_{11}} & \frac{1-d_2}{E_{22}} & -\frac{\nu_{32}}{E_{33}} & 0 & 0 & 0 \\ -\frac{\nu_{13}}{E_{11}} & -\frac{\nu_{23}}{E_{22}} & \frac{1-d_3}{E_{33}} & 0 & 0 & 0 \\ 0 & 0 & 0 & \frac{(1-d_4)(1+\nu_{12})}{E_{22}} & 0 & 0 \\ 0 & 0 & 0 & 0 & \frac{1-d_5}{G_{31}} & 0 \\ 0 & 0 & 0 & 0 & 0 & \frac{1-d_6}{G_{12}} \end{bmatrix} \tag{49}$$

The evolution of damage in 3D space is based on the evolution of strain in corresponding 1D direction according to 7 and expressed as

$$(1-d_i)E_i = \frac{\sigma_i}{\varepsilon_i} \tag{50}$$

$$d_i = 1 - \frac{\sigma_i}{E_i \varepsilon_i} \tag{51}$$

$$\varepsilon_{0,i} - \varepsilon_{E,i} = \frac{2G_{f,i}}{f_{0,i} l_i} \tag{52}$$

$$\sigma_i = \frac{f_{0,i}(\varepsilon_{0,i} - \varepsilon_i)}{(\varepsilon_{0,i} - \varepsilon_{E,i})} = f_{0,i} - \frac{f_{0,i}^2 l_i}{2G_{f,i}}(\varepsilon_i - \varepsilon_{E,i}) \tag{53}$$

where $\varepsilon_{0,i}$ is strain at zero stress, $f_{0,i}$ is maximum given stress, $\varepsilon_{E,i}$ is strain at maximum stress, $G_{f,i}$ is fracture energy disregarding the characteristic size of finite element, l_i is the characteristic length associated with element size and interpolation order. The solution is similar to section and proceeds in total strain and strees formulation. Fig. 8 shows a typical performance for damage in one direction.

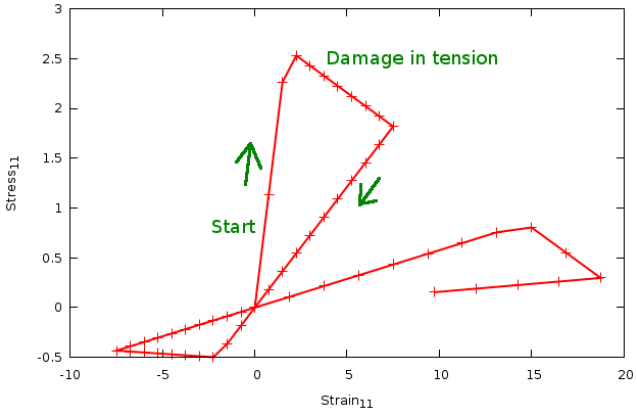

Figure 8: Typical loading/unloading material performance for homogenized stress and strain in direction$_{11}$. Note that damage parameter is common for tension and compression.

Description	Material for composite brittle damage
Record Format	**compdammat** num$_{(in)}$ # d$_{(rn)}$ # Exx$_{(rn)}$ # EyyEzz$_{(rn)}$ # nuxynuxz$_{(rn)}$ # nuyz$_{(rn)}$ # GxyGxz$_{(rn)}$ # [Tension_f0_Gf$_{(rn)}$ #] [Compres_f0_gf$_{(rn)}$ #]
Parameters	- *num* material model number - *d* material density - *Exx* Young's modulus for principal direction xx - *EyyEzz* Young's modulus in othogonal directions to the principal direction xx - *nuxynuxz* Poisson's ratio in xy and xz directions - *nuyz* Poisson's ratio in yz direction - *GxyGxz* shear modulus in xy and xz directions - *Tension_f0_Gf* array with six pairs of positive numbers. Each pair desribes maximum stress in tension and fracture energy for each direction (xx, yy, zz, yz, zx, xy) - *Compres_f0_gf* array with six pairs of numbers. Each pair desribes maximum stress in compression (given as a negative number) and positive fracture energy for each direction (xx, yy, zz, yz, zx, xy)
Supported modes	3dMat, 1dMat

Table 21: Brittle damage for composites - summary.

2 Material Models for Transport Problems

2.1 Isotropic Linear Material

Linear isotropic material model for transport problems. The model parameters are summarized in table 22.

Description	Linear isotropic elastic material
Record Format	**IsoHeat** num(in) # d(rn) # k(rn) # c(rn) #
Parameters	- *num* material model number
	- *d* material density
	- *k* Conductivity
	- *n* Specific heat
Supported modes	_2dHeat

Table 22: Linear Isotropic Material - summary.

2.2 Coupled heat and mass transfer material model

Coupled heat and mass transfer material model. Source: T. Krejci doctoral thesis; Bazant and Najjar, 1972; Pedersen, 1990. Assumptions:water vapor is the only driving mechanism; relative humidity is from range 0.2 - 0.98 (I and II regions). The model parameters are summarized in table 23.

Description	Coupled heat and mass transfer material model
Record Format	**HeMotk** num$_{(in)}$ # d$_{(rn)}$ # a_0$_{(rn)}$ # nn$_{(rn)}$ # phi_c$_{(rn)}$ # delta_wet$_{(rn)}$ # w_h$_{(rn)}$ # n$_{(rn)}$ # a$_{(rn)}$ # latent$_{(rn)}$ # c$_{(rn)}$ # rho$_{(rn)}$ # chi_eff$_{(rn)}$ # por$_{(rn)}$ # rho_gws$_{(rn)}$ #
Parameters	- *num* material model number - *d*, *rho* material density - *a_0* constant (obtained from experiments) a_0 [Bazant and Najjar, 1972] - *nn* constant-exponent (obtained from experiments) n [Bazant and Najjar, 1972] - *phi_c* constant-relative humidity (obtained from experiments) phi_c [Bazant and Najjar, 1972] - *delta_wet* constant-water vapor permeability (obtained from experiments) delta_wet [Bazant and Najjar, 1972] - *w_h* constant water content (obtained from experiments) w_h [Pedersen, 1990] - *n* constant-exponent (obtained from experiments) n [Pedersen, 1990] - *a* constant (obtained from experiments) A [Pedersen, 1990] - *latent* latent heat of evaporation - *c* thermal capacity - *chi_eff* effective thermal conductivity - *por* porosity - *rho_gws* saturation volume density
Supported modes	_2dHeMo

Table 23: Coupled heat and mass transfer material model - summary.

3 Material Models for Fluid Dynamic

3.1 Newtonian Fluid

Constitutive model of Newtonian fluid. The model parameters are summarized in table 24.

Description	Newtonian Fluid material
Record Format	**NewtonianFluid** num$_{(in)}$ # d$_{(rn)}$ # mu$_{(rn)}$ #
Parameters	- *num* material model number
	- *d* material density
	- *mu* viscosity
Supported modes	2dFlow

Table 24: Newtonian Fluid material - summary.

3.2 Bingham Fluid

Constitutive model of Bingham fluid. This is a constitutive model of non-Newtonian type. The model parameters are summarized in table 25.

In the Bingham model the flow is characterized by following constitutive equation

$$\boldsymbol{\tau} = \boldsymbol{\tau}_0 + \mu\dot{\boldsymbol{\gamma}} \quad \text{if } \dot{\tau} \geq \tau_0 \tag{54}$$

$$\dot{\gamma} = \mathbf{0} \quad \text{if } \dot{\tau} \leq \tau_0 \tag{55}$$

where $\boldsymbol{\tau}$ is the shear stress applied to material, $\dot{\tau} = \sqrt{\boldsymbol{\tau} : \boldsymbol{\tau}}$ is the shear stress measure, $\dot{\boldsymbol{\gamma}}$ is the shear rate, $\boldsymbol{\tau}_0$ is the yield stress, and μ is the plastic viscosity. The parameters for the model can be in general determined using two possibilities: (i) stress controlled rheometer, when the stress is applied to material and shear rate is measured, and (ii) shear rate controlled rheometer, where concrete is sheared and stress is measured. However, most of the widely used tests are unsatisfactory in the sense, that they measure only one parameter. These one-factor tests include slump test, penetrating rod test, and Ve-Be test. Recently, some tests providing two parameters on output have been designed (BTRHEOM, IBB, and BML rheometers). Also a refined version of the standard slump test has been developed for estimating yield stress and plastic viscosity. The test is based on measuring the time necessary for the upper surface of the concrete cone in the slump to fall a distance 100 mm. Semi-empirical models are then proposed for estimating yield stress and viscosity based on measured results. The advantage is, that this test does not require any special equipment, provided that the one for the standard version is available.

In order to avoid numerical difficulties caused by the existence of the sharp angle in material model response at $\tau = \tau_0$, the numerical implementation uses following smoothed relation for viscosity

$$\mu = \mu_0 + \frac{\tau_0}{\dot{\gamma}}(1 - e^{-m\dot{\gamma}}) \tag{56}$$

where m is so called stress growth parameter. The higher value of parameter m, the closer approximation of the original constitutive equation (54) is obtained.

Description	Bingham fluid material
Record Format	**BinghamFluid** num$_{(in)}$ # d$_{(rn)}$ # mu0$_{(rn)}$ # tau0$_{(rn)}$ #
Parameters	- *num* material model number - *d* material density - *mu0* viscosity - *tau0* Yield stress
Supported modes	_2dFlow

Table 25: Bingham Fluid material - summary.

3.3 Two-Fluid material

Material coupling the behaviour of two particulat materials based on rule of mixture. The weighting factor is VOF fraction. The model parameters are summarized in table 26.

Description	Two-Fluid material
Record Format	**twofluidmat** num$_{(in)}$ # mat$_{(ia)}$ #
Parameters	- *num* material model number - *mat* integer array contaning two numbers representing numbers of material models of which the receiver is composed. Material with index 0 is a material, that is fully active in a cell with VOF=0, material with index 1 is a material fuully active in a cell with VOF=1.
Supported modes	_2dFlow

Table 26: Two-Fluid material - summary.

4 Material drivers - theory & application

The purpose of this section is to present the theoretical backgroung of some handy general purpose algorithms, that are provided in oofem in the form of general material base classes. They can significantly facilitate the implementation of particular material models that are based on such concepts. Typical example can be a general purpose plasticity class, that implements general stress return and stifness matrix evaluation algorithms, based on provided methods for computing yield functions and corresponding derivatives. Particular models are simply derived from the base classes, inheriting common algorithms.

4.1 Multisurface plasticity driver - MPlasticMaterial class

In this section, a general multisurface plasticity theory with hardening/softening is reviewed. The presented algorithms are implemented in MPlasticMaterial class.

4.1.1 Plasticity overview

Let $\boldsymbol{\sigma}, \boldsymbol{\varepsilon}$, and $\boldsymbol{\varepsilon}^p$ be the stress, total strain, and plastic strain vectors, respectively. It is assumed that the total strain is decomposed into reversible elastic and irreversible plastic parts

$$\boldsymbol{\varepsilon} = \boldsymbol{\varepsilon}^e + \boldsymbol{\varepsilon}^p \tag{57}$$

The elastic response is characterized in terms of elastic constitutive matrix $\boldsymbol{D}$ as

$$\boldsymbol{\sigma} = \boldsymbol{D}\boldsymbol{\varepsilon}^e = \boldsymbol{D}(\boldsymbol{\varepsilon} - \boldsymbol{\varepsilon}^p) \tag{58}$$

As long as the stress remains inside the elastic domain, the deformation process is purely elastic and the plastic strain does not change. It is assumed that the elastic domain, denoted as IE is bounded by a composite yield surface. It is defined as

$$IE = \{(\boldsymbol{\sigma}, \boldsymbol{\kappa}) | f_i(\boldsymbol{\sigma}, \boldsymbol{\kappa}) < 0, \text{for all i} \in \{1, \cdots, \text{m}\}\} \tag{59}$$

where $f_i(\boldsymbol{\sigma}, \boldsymbol{\kappa})$ are $m \geq 1$ yield functions intersecting in a possibly non-smooth fashion. The vector $\boldsymbol{\kappa}$ contains internal variables controlling the evolution of yield surfaces (amount of hardening or softening). The evolution of plastic strain $\boldsymbol{\varepsilon}^p$ is expressed in Koiter's form. Assuming the non-associated plasticity, this reads

$$\dot{\boldsymbol{\varepsilon}}^p = \sum_{i=1}^{m} \lambda^i \partial_{\boldsymbol{\sigma}} g_i(\boldsymbol{\sigma}, \boldsymbol{\kappa}) \tag{60}$$

where g_i are plastic potential functions. The λ^i are referred as plastic consistency parameters, which satisfy the following Kuhn-Tucker conditions

$$\lambda^i \geq 0, \ f_i \leq 0, \text{ and } \lambda^i f_i = 0 \tag{61}$$

These conditions imply that in the elastic regime the yield function must remain negative and the rate of the plastic multiplier is zero (plastic strain remains constant) while in the plastic regime the yield function must be equal to zero (stress remains on the surface) and the rate of the plastic multiplier is positive.

The evolution of vector of internal hardening/softening variables $\boldsymbol{\kappa}$ is expressed in terms of a general hardening/softening law of the form

$$\dot{\boldsymbol{\kappa}} = \dot{\boldsymbol{\kappa}}(\boldsymbol{\sigma}, \boldsymbol{\lambda}) \tag{62}$$

where $\boldsymbol{\lambda}$ is the vector of plastic consistency parameters λ_i.

4.1.2 Closest point return algorithm

Let us assume, that at time t_n the total and plastic strain vectors and internal variables are known

$$\{\boldsymbol{\varepsilon}_n, \boldsymbol{\varepsilon}^p_n, \boldsymbol{\kappa}_n\} \text{ given at } t_n$$

By applying an implicit backward Euler difference scheme to the evolution equations (58 and 60) and making use of the initial conditions the following discrete non-linear system is obtained

$$\begin{aligned}
\boldsymbol{\varepsilon}_{n+1} &= \boldsymbol{\varepsilon}_n + \Delta\boldsymbol{\varepsilon} && (63)\\
\boldsymbol{\sigma}_{n+1} &= \boldsymbol{D}(\boldsymbol{\varepsilon}_{n+1} - \boldsymbol{\varepsilon}^p_{n+1}) && (64)\\
\boldsymbol{\varepsilon}^p_{n+1} &= \boldsymbol{\varepsilon}^p_n + \sum \lambda^i \partial_{\boldsymbol{\sigma}} g_i(\boldsymbol{\sigma}_{n+1}, \boldsymbol{\kappa}_{n+1}) && (65)
\end{aligned}$$

In addition, the discrete counterpart of the Kuhn-Tucker conditions becomes

$$\begin{aligned}
f_i(\boldsymbol{\sigma}_{n+1}, \boldsymbol{\kappa}_{n+1}) &= 0 && (66)\\
\lambda^i_{n+1} &\geq 0 && (67)\\
\lambda^i_{n+1} f_i(\boldsymbol{\sigma}_{n+1}, \boldsymbol{\kappa}_{n+1}) &= 0 && (68)
\end{aligned}$$

In the standard displacement-based finite element analysis, the strain evolution is determined by the displacement increments computed on the structural level. The basic task on the level of a material point is to evaluate the stress evolution generated by strain history. According to this, the strain driven algorithm is assumed, i.e. that the total strain $\boldsymbol{\varepsilon}_{n+1}$ is given. Then, the Kuhn-Tucker conditions determine whether a constraint is active. The set of active constraints is denoted as J_{act} and is defined as

$$J_{act} = \{\beta \in \{1, \cdots, m\} | f_\beta = 0 \ \& \ \dot{f}_\beta = 0\} \tag{69}$$

Let's start with the definition of the residual of plastic flow

$$\boldsymbol{R}_{n+1} = -\boldsymbol{\varepsilon}^p_{n+1} + \boldsymbol{\varepsilon}^p_n + \sum_{j \in J_{act}} \lambda^j_{n+1} \partial_\sigma g_{n+1} \tag{70}$$

By noting that total strain $\boldsymbol{\varepsilon}_{n+1}$ is fixed during the increment we can express the plastic strain increment using (58) as

$$\Delta\boldsymbol{\varepsilon}^p_{n+1} = -\boldsymbol{D}\Delta\boldsymbol{\sigma}_{n+1} \tag{71}$$

The linearization of the plastic flow residual (70) yields[2]

$$\begin{aligned}
&\boldsymbol{R} + \boldsymbol{D}^{-1}\Delta\boldsymbol{\sigma} + \sum \lambda \partial_{\sigma\sigma} g \Delta\boldsymbol{\sigma} + \\
&+ \sum \lambda \partial_{\sigma\kappa} g \cdot (\partial_\sigma \kappa \Delta\boldsymbol{\sigma} + \partial_\lambda \kappa \Delta\lambda) + \sum \Delta\lambda \partial_\sigma g = 0
\end{aligned} \tag{72}$$

[2]For brevity, the simplified notation is introduced: $f = f(\boldsymbol{\sigma}, \boldsymbol{\kappa})$, $g = g(\boldsymbol{\sigma}, \boldsymbol{\kappa})$, $\boldsymbol{\kappa} = \boldsymbol{\kappa}(\boldsymbol{\sigma}, \lambda)$, and subscript $n+1$ is omitted.

From the previous equation, the stress increment $\Delta\boldsymbol{\sigma}$ can be expressed as

$$\Delta\boldsymbol{\sigma} = -\boldsymbol{H}^{-1}\left(\boldsymbol{R} + \sum \Delta\lambda\partial_\sigma g + \sum \lambda\partial_{\sigma\kappa} g\partial_\lambda\kappa\Delta\lambda\right) \tag{73}$$

where $\boldsymbol{H}$ is algorithmic moduli defined as

$$\boldsymbol{H} = \left[\boldsymbol{D}^{-1} + \sum \lambda\partial_{\sigma\sigma} g + \sum \lambda\partial_{\sigma\kappa} g\partial_\sigma\kappa\right] \tag{74}$$

Differentiation of active discrete consistency conditions (66) yields

$$\boldsymbol{f} + \partial_\sigma \boldsymbol{f}\Delta\boldsymbol{\sigma} + \partial_\kappa \boldsymbol{f}(\partial_\sigma\kappa\Delta\boldsymbol{\sigma} + \partial_\lambda\kappa\Delta\lambda) = 0 \tag{75}$$

Finally, by combining equations (73) and (75), one can obtain expression for incremental vector of consistency parameters $\Delta\boldsymbol{\lambda}$

$$\left[\boldsymbol{V}^T\boldsymbol{H}^{-1}\boldsymbol{U} - \partial_\kappa \boldsymbol{f}\partial_\lambda\boldsymbol{\kappa}\right]\Delta\boldsymbol{\lambda} = \boldsymbol{f} - \boldsymbol{V}^T\boldsymbol{H}^{-1}\boldsymbol{R} \tag{76}$$

where the matrices $\boldsymbol{U}$ and $\boldsymbol{V}$ are defined as

$$\boldsymbol{U} = \left[\partial_\sigma \boldsymbol{g} + \sum \lambda\partial_{\sigma\kappa} g\partial_\lambda\kappa\right] \tag{77}$$

$$\boldsymbol{V} = [\partial_\sigma \boldsymbol{f} + \partial_\kappa \boldsymbol{f}\partial_\sigma\kappa] \tag{78}$$

Before presenting the final return mapping algorithm, the algorithm for determination of the active constrains should be discussed. A yield surface $f_{i,n+1}$ is active if $\lambda^i_{n+1} > 0$. A systematic enforcement of the discrete Kuhn-Tucker condition (66), which relies on the solution of return mapping algorithm, then serves as the basis for determining the active constraints. The starting point in enforcing (66) is to define the trial set

$$J^{trial}_{act} = \{j \in \{1, \cdots, m\} | f^{trial}_{j,n+1} > 0\} \tag{79}$$

where $J_{act} \subseteq J^{trial}_{act}$. Two different procedures can be adopted to determine the final set J_{act}. The conceptual procedure is as follows

- Solve the closest point projection with $J_{act} = J^{trial}_{act}$ to obtain final stresses, along with $\lambda^i_{n+1},\ i \in J^{trial}_{act}$.
- Check the sign of λ^i_{n+1}. If $\lambda^i_{n+1} < 0$, for some $i \in J^{trial}_{act}$, drop the $i-$th constrain from the active set and goto first point. Otherwise exit.

In the procedure 2, the working set J^{trial}_{act} is allowed to change within the iteration process, as follows

- Let $J^{(k)}_{act}$ be the working set at the k-th iteration. Compute increments $\Delta\lambda^{i,(k)}_{n+1},\ i \in J^{(k)}_{act}$.
- Update and check the signs of $\Delta\lambda^{i,(k)}_{n+1}$. If $\Delta\lambda^{i,(k)}_{n+1} < 0$, drop the i-th constrain from the active set $J^{(k)}_{act}$ and restart the iteration. Otherwise continue with next iteration.

If the consistency parameters $\Delta\lambda^i$ can be shown to increase monotonically within the return mapping algorithm, the the latter procedure is preferred since it leads to more efficient computer implementation.

The overall algorithm is convergent, first order accurate and unconditionally stable. The general algorithm is summarized in table (4.1.2).

1. Elastic predictor

   (a) Compute Elastic predictor (assume frozen plastic flow)
   $\boldsymbol{\sigma}_{n+1}^{trial} = \boldsymbol{D}\left(\boldsymbol{\varepsilon}_{n+1} - \boldsymbol{\varepsilon}_n^p\right)$
   $f_{i,n+1}^{trial} = f_i(\boldsymbol{\sigma}_{n+1}^{trial}, \boldsymbol{\kappa}_n),$ for i $\in \{1, \cdots, \mathrm{m}\}$

   (b) Check for plastic processes IF $f_{i,n+1}^{trial} \leq 0$ for all $i \in \{1, \cdots, m\}$ THEN:

   Trial state is the final state, EXIT.

   ELSE:

   $J_{act}^{(0)} = \{i \in \{1, \cdots, m\} | f_{i,n+1}^{trial} > 0\}$
   $\boldsymbol{\varepsilon}_{n+1}^{p(0)} = \boldsymbol{\varepsilon}_n^p,\ \boldsymbol{\kappa}_{n+1}^{(0)} = \boldsymbol{\kappa}_n,\ \lambda_{n+1}^{i(0)} = 0$

   ENDIF

2. Plastic Corrector

   (c) Evaluate plastic strain residual

   $\boldsymbol{\sigma}_{n+1}^{(k)} = \boldsymbol{D}\left(\boldsymbol{\varepsilon}_{n+1} - \boldsymbol{\varepsilon}_{n+1}^{p(k)}\right)$
   $\boldsymbol{R}_{n+1}^{(k)} = -\boldsymbol{\varepsilon}_{n+1}^{p(k)} + \boldsymbol{\varepsilon}_n^p + \sum \lambda_{n+1}^{i(k)} \partial_\sigma g_i$

   (d) Check convergence

   $f_{i,n+1}^{(k)} = f_i(\boldsymbol{\sigma}_{n+1}^{(k)}, \boldsymbol{\kappa}_{n+1}^{(k)})$
   if $f_{i,n+1}^{(k)} < TOL$, for all $i \in J_{act}^{(k)}$ and $\|\boldsymbol{R}_{n+1}^{(k)}\| < TOL$ then EXIT

   (e) Compute consistent moduli

   $\boldsymbol{G} = \left[\boldsymbol{V}^T \boldsymbol{H}^{-1} \boldsymbol{U} - \partial_\kappa \boldsymbol{f} \partial_\lambda \boldsymbol{\kappa}\right]^{-1}$

   (f) Obtain increments to consistency parameter

   $\Delta\boldsymbol{\lambda}_{n+1}^{(k)} = \boldsymbol{G}\{\boldsymbol{f} - \boldsymbol{V}^T \boldsymbol{H}^{-1} \boldsymbol{R}\}_{n+1}^{(k)}$
   If using procedure 2 to determine active constrains, then update the active set and restart iteration if necessary

   (g) Obtain increments of plastic strains and internal variables

   $\Delta\boldsymbol{\varepsilon}_{n+1}^{p(k)} = \boldsymbol{D}^{-1}\left\{\boldsymbol{R}_{n+1}^{(k)} + \sum \Delta\lambda_{n+1}^{i(k)} \partial_\sigma g_{n+1}^{(k)} + \sum \lambda_{n+1}^{i(k)} \partial_{\sigma\kappa} g_{n+1}^{(k)} \partial_\lambda \kappa \Delta\lambda_{n+1}^{i(k)}\right\}$
   $\Delta\boldsymbol{\kappa}_{n+1}^{(k)} = \dot{\boldsymbol{\kappa}}(\boldsymbol{\sigma}^{(k)_{n+1}}, \boldsymbol{\lambda}_{n+1}^k)$

   (h) Update state variables

   $\boldsymbol{\varepsilon}_{n+1}^{p(k+1)} = \boldsymbol{\varepsilon}_{n+1}^{p(k)} + \Delta\boldsymbol{\varepsilon}_{n+1}^{p(k)}$
   $\boldsymbol{\kappa}_{n+1}^{(k+1)} = \boldsymbol{\kappa}_{n+1}^{(k)} + \Delta\boldsymbol{\kappa}_{n+1}^{(k)}$
   $\lambda_{n+1}^{i(k+1)} = \lambda_{n+1}^{i(k)} + \Delta\boldsymbol{\lambda}_{n+1}^{(k)},\ i \in J_{act}$

   (i) Set k=k+1 and goto step (b)

Table 27: General multisurface closest point algorithm

4.1.3 Algorithmic stiffness

Differentiation of the elastic stress-strain relations (64) and the discrete flow rule (65) yields

$$d\boldsymbol{\sigma}_{n+1} = \boldsymbol{D}\left(d\boldsymbol{\varepsilon}_{n+1} - d\boldsymbol{\varepsilon}_{n+1}^p\right) \tag{80}$$

$$d\boldsymbol{\varepsilon}^p_{n+1} = \sum \left(\lambda^i \partial_{\sigma\sigma} g d\boldsymbol{\sigma} + \lambda^i \partial_{\sigma\kappa} g \left(\partial_\sigma \boldsymbol{\kappa} d\boldsymbol{\sigma} + \partial_\lambda \boldsymbol{\kappa} d\lambda^i\right) + d\lambda^i \partial_\sigma g\right) \quad (81)$$

Combining this two equations, one obtains following relation

$$d\boldsymbol{\sigma} = \boldsymbol{\Xi}_{n+1} \left\{ d\boldsymbol{\varepsilon}_{n+1} - \sum \lambda^i \partial_{\sigma\kappa} g \partial_\lambda \boldsymbol{\kappa} d\lambda^i - \sum d\lambda^i \partial_\sigma g \right\} \quad (82)$$

where $\boldsymbol{\Xi}_{n+1}$ is the algorithmic moduli defined as

$$\boldsymbol{\Xi}_{n+1} = \left[\boldsymbol{D}^{-1} + \sum \lambda^i \partial_{\sigma\sigma} g + \sum \lambda \partial_{\sigma\kappa} g \partial_\sigma \boldsymbol{\kappa} \right] \quad (83)$$

Differentiation of discrete consistency condition yields

$$\partial_\sigma f^i d\boldsymbol{\sigma} + \partial_\kappa f^i (\partial_\sigma \boldsymbol{\kappa} d\boldsymbol{\sigma} + \partial_\lambda \boldsymbol{\kappa} d\boldsymbol{\lambda}) = 0 \quad (84)$$

By substitution of (82) into (84) the following relation is obtained

$$d\boldsymbol{\lambda} = \boldsymbol{G} \left\{ \boldsymbol{V} \boldsymbol{\Xi} d\boldsymbol{\varepsilon} \right\} \quad (85)$$

where matrix $\boldsymbol{G}$ is defined as

$$\boldsymbol{G} = \left[\boldsymbol{V}^T \boldsymbol{\Xi} \boldsymbol{U} - \partial_\kappa \boldsymbol{f} \partial_\lambda \boldsymbol{\kappa} \right]^{-1} \quad (86)$$

Finally, by substitution of (86) into (82) one obtains the algorithmic elastoplastic tangent moduli

$$\frac{\mathrm{d}\boldsymbol{\sigma}}{\mathrm{d}\boldsymbol{\varepsilon}}|_{n+1} = \boldsymbol{\Xi} - \boldsymbol{\Xi} \boldsymbol{U} \left(\boldsymbol{V} \boldsymbol{\Xi} \boldsymbol{U} - [\partial_\kappa f][\partial_\lambda \boldsymbol{\kappa}] \right) \boldsymbol{V} \boldsymbol{\Xi} \quad (87)$$

4.1.4 Implementation of particular models

As follows from previous sections, a new plasticity based class has to provide only some model-specific services. The list of services, that should be implemented includes (for full reference, please consult documentation of MPlasticMaterial class):

- method for computing the value of yield function (computeYieldValueAt service)
- method for computing stress gradients of yield and load functions (method computeStressGradientVector)
- method for computing hardening variable gradients of yield and load functions (method computeKGradientVector)
- methods for computing gradient of hardening variables with respect to stress and plastic multipliers vectors (computeReducedHardeningVarsSigmaGradient and computeReducedHardeningVarsLamGradient methods)
- method for evaluating the increments of hardening variables due to reached state (computeStrainHardeningVarsIncrement)
- methods for computing second order derivatives of load and yield functions (computeReducedSSGradientMatrix and computeReducedSKGradientMatrix methods). Necessary only if consistent stiffness is required.

4.2 Isotropic Damage Model - IsotropicDamageMaterial class

1.5 In this section, the implementation of an isotropic damage model will be described. To cover the various models based on isotropic damage concept, a base class IsotropicDamageMaterial is defined first, declaring the necessary services and providing the implementation of them, which are general. The derived classes then only implement a particular damage-evolution law.

The isotropic damage models are based on the simplifying assumption that the stiffness degradation is isotropic, i.e., stiffness moduli corresponding to different directions decrease proportionally and independently of direction of loading. Consequently, the damaged stiffness matrix is expressed as

$$\boldsymbol{D} = (1-\omega)\boldsymbol{D}_e,$$

where $\boldsymbol{D}_e$ is elastic stiffness matrix of the undamaged material and ω is the damage parameter. Initially, ω is set to zero, representing the virgin undamaged material, and the response is linear-elastic. As the material undergoes the deformation, the initiation and propagation of microdefects decreases the stiffness, which is represented by the growth of the damage parameter ω. For $\omega = 1$, the stiffness completely disappears.

In the present context, the $\boldsymbol{D}$ matrix represents the secant stiffness that relates the total strain to the total stress

$$\boldsymbol{\sigma} = \boldsymbol{D}\boldsymbol{\varepsilon} = (1-\omega)\boldsymbol{D}_e\boldsymbol{\varepsilon}.$$

Similarly to the theory of plasticity, a loading function f is introduced. In the damage theory, it is natural to work in the strain space and therefore the loading function is depending on the strain and on an additional parameter κ, describing the evolution of the damage. Physically, κ is a scalar measure of the largest strain level ever reached. The loading function usually has the form

$$f(\boldsymbol{\varepsilon}, \kappa) = \tilde{\varepsilon}(\boldsymbol{\varepsilon}) - \kappa,$$

where $\tilde{\varepsilon}$ is the equivalent strain, i.e., the scalar measure of the strain level. Damage can grow only if current state reaches the boundary of elastic domain ($f = 0$). This is expressed by the following loading/unloading conditions

$$f \leq 0, \quad \dot{\kappa} \geq 0, \quad \dot{\kappa} f = 0.$$

It remains to link the variable κ to the damage parameter ω. As both κ and ω grow monotonically, it is convenient to postulate an explicit evolution law

$$\omega = g(\kappa).$$

The important advantage of this explicit formulation is that the stress corresponding to the given strain can be evaluated directly, without the need to solve the nonlinear system of equations. For the given strain, the corresponding stress is computed simply by evaluating the current equivalent strain, updating the maximum previously reached equivalent strain value κ and the damage parameter and reducing the effective stress according to $\boldsymbol{\sigma} = (1-\omega)\boldsymbol{D}_e\boldsymbol{\varepsilon}$.

This general framework for computing stresses and stiffness matrix is common for all material models of this type. Therefore, it is natural to introduce

the base class for all isotropic-based damage models which provides the general implementation for the stress and stiffness matrix evaluation algorithms. The particular models then only provide their equivalent strain and damage evolution law definitions. The base class only declares the virtual services for computing equivalent strain and corresponding damage. The implementation of common services uses these virtual functions, but they are only declared at IsotropicDamageMaterial class level and have to be implemented by the derived classes.

Together with the material model, the corresponding status has to be defined, containing all necessary history variables. For the isotropic-based damage models, the only history variable is the value of the largest strain level ever reached (κ). In addition, the corresponding damage level ω will be stored. This is not necessary because damage can be always computed from corresponding κ. The IsotropicDamageMaterialStatus class is derived from StructuralMaterialStatus class. The base class represents the base material status class for all structural statuses. At StructuralMaterialStatus level, the attributes common to all "structural analysis" material models - the strain and stress vectors (both the temporary and non-temporary) are introduced. The corresponding services for accessing, setting, initializing, and updating these attributes are provided. Therefore, only the κ and ω parameters are introduced (both the temporary and non-temporary). The corresponding services for manipulating these attributes are added and services for context initialization, update, and store/restore operations are overloaded, to handle the history parameters properly.

References

[1] M. Jirásek, Z.P. Bažant: Inelastic analysis of structures, John Wiley, 2001.

[2] Jirásek, M.: Comments on microplane theory, Mechanics of Quasi-Brittle Materials and Structures, ed. G. Pijaudier-Cabot, Z. Bittnar, and B. Gérard, Hermès Science Publications, Paris, 1999, pp. 57-77.

[3] B. Patzák: OOFEM home page, http://www.oofem.org, 2003.

[4] M. Ortiz, E.P. Popov: Accuracy and stability of integration algorithms for elasto-plastic constitutive relations, Int. J. Numer. Methods Engrg, 21, 1561-1576, 1985.

[5] J.C. Simo, J.G. Kennedy, S. Govindjee: Non-smooth multisurface plasticity and viscoplasticity. Loading/unloading conditions and numerical algorithms, Int. J. Numer. Methods Engrg, 26, 2161-2185, 1988.

[6] B.Lourenco, J.G. Rots: Multisurface Interface Model for Analysis of Masonry Structures, Journal of Engng Mech, vol. 123, No. 7, 1997.

[7] Z.P. Bažant, J. Planas: Fracture and Size Effect in Concrete and Other Quasibrittle Materials, CRC Press, 1998.